Structural Properties of $Ni_{3+x}Sn_4$

Sigrid Furuseth[a,*] and Helmer Fjellvåg[b]

[a]Department of Chemistry, University of Oslo, Blindern, N-0315 Oslo 3 and [b]Institute for Energy Technology, N-2007 Kjeller, Norway

Furuseth, S. and Fjellvåg, H., 1986. Structural Properties of $Ni_{3+x}Sn_4$. – Acta Chem. Scand. A 40: 695–700.

The $Ni_{3+x}Sn_4$ phase exists for $0.080 \pm 0.005 \leqq x \leqq 0.60 \pm 0.02$ at room temperature. The homogeneity range is strongly temperature-dependent. The variable composition results from partial filling of the 2(*c*) position (spacegroup *C2/m*) by Ni atoms. The crystal structure contains fragments of the NiAs-type structure and units related to the $NiBi_3$-type structure, and is closely related to that of CoGe and $Ni_{7+y}Sn_8$. No phase transition occurs between room temperature and the temperature of decomposition.

A total of four binary phases[1-3] have been reported and structurally characterized for the Ni–Sn system. Of these, Ni_3Sn_4 constitutes the most tin-rich phase. This phase is often encountered, as powder or single crystals, in tin flux experiments on the crystal growth of various nickel (binary or ternary) phases, and the availability of detailed information on the crystal structure properties of Ni_3Sn_4 is therefore of value.

The homogeneity range and the crystal structure of Ni_3Sn_4 have been described by various research groups. However, in this study additional information on its structural properties between 300 and 1100 K has been obtained by means of powder and single crystal X-ray diffraction measurements. As a natural extension, some results for the closely related NiSn phase are also included.

Experimental

Powder samples with compositions $Ni_{3+x}Sn_4$, $0 < x < 1$, were synthesized from the elements (Ni, turnings from rods, 99.99 %, Johnson Matthey, and Sn, granules 99.9 %, Fluka AG) by heating weighed amounts in sealed, evacuated silica tubes. After an initial heat-treatment at 950 °C for 1 d followed by 3 d at 700 °C, the samples were cooled to room temperature and crushed. The samples were subjected to a second annealing for 1 wk; they were then quenched in ice-water from temperatures between 600 and 800 °C, or were slowly cooled (over 8 d) to room temperature. The homogeneity and the structural state of the samples were deduced from powder X-ray diffraction data recorded at room temperature (Guinier camera, Cu$K\alpha_1$ radiation, Si as internal standard). Unit cell dimensions were derived by least-squares refinement using the CELLKANT[4] program. High temperature powder X-ray diffraction data were collected between 300 and 1100 K with a Guinier Simon camera (Enraf-Nonius, Cu$K\alpha_1$ radiation).

Magnetic susceptibility was measured by the Faraday method between 80 and 1000 K (maximum field strength 8 kØ). Single crystals of the Ni_3Sn_4 phase were obtained by prolonged heating (8–14 d) of samples with a surplus of tin (molar ratio Ni:Sn ~ 1:3), followed by either quenching from 700 °C or slow cooling to room temperature over a period of 2 wk. Excess of tin was removed by dissolution in hydrochloric acid, leaving single crystals of dimensions up to 1×0.2×0.2 mm, the largest ones being obtained with slowly-cooled samples. The compositions of the crystals were established by comparing the refined unit cell

*To whom correspondence should be addressed.

Table 1. Crystallographic data for $Ni_{3.08}Sn_4$ and $Ni_{3.39}Sn_4$.

	$Ni_{3.08}Sn_4$	$Ni_{3.39}Sn_4$
Space group	*C*2/*m*	*C*2/*m*
a/pm	1219.9(2)	1237.1(2)
b/pm	406.09(5)	406.90(6)
c/pm	522.38(7)	521.00(7)
β/°	105.17(1)	104.06(1)
$V/10^6$ pm^3	249.76(6)	254.40(6)
Z	2	2
d_x/g cm^{-3}	8.716(2)	8.795(2)
Obsd. reflections	1062	1092
R/%	2.6	3.7
R_w/%	3.6	6.5

dimensions with corresponding values obtained from powder diffraction data for a series of samples of varying composition.

Intensity data collection and refinement. Two single crystals with compositions $Ni_{3.39}Sn_4$ (quenched from 700 °C) and $Ni_{3.08}Sn_4$ (cooled slowly), respectively, were ground to spheres of diam. ~0.15 mm. Intensity data were recorded at room temperature with a Nicolet P3/F diffractometer by the ω/2θ scan technique using Mo*K*α radiation (λ = 71.069 pm). Intensity data were collected up to 2θ = 90°, with a scan speed of 4° min^{-1}. Only reflections with $I > 3\sigma(I)$ were considered observed. Corrections were made for Lorentz and polarization effects, absorption and isotropic extinction. Full matrix least-squares refinements were performed according to the programs described in Refs. 5 and 6, and the weighting adopted was $w = 1/\sigma^2(F_{obs})$.

Results and discussion

$Ni_{3+x}Sn_4$ is found, both from powder and single crystal X-ray diffraction data, to possess a monoclinic unit cell, in accordance with earlier findings.[1] The $Ni_{3+x}Sn_4$ phase exhibits a rather broad, temperature-dependent homogeneity range. The variations in the unit cell dimensions as a function of *x* for samples cooled slowly to room temperature are shown in Fig. 1. While *a*, *b* and *V* increase with increasing Ni content (*x*), a slight decrease occurs for *c* and β. At 295 K the $Ni_{3+x}Sn_4$ phase covers the composition range $0.080 \pm 0.005 \leqq x \leqq 0.60 \pm 0.02$ (samples with $x = 0.00$ and 0.70 show additional reflections from Sn and NiSn, respectively).

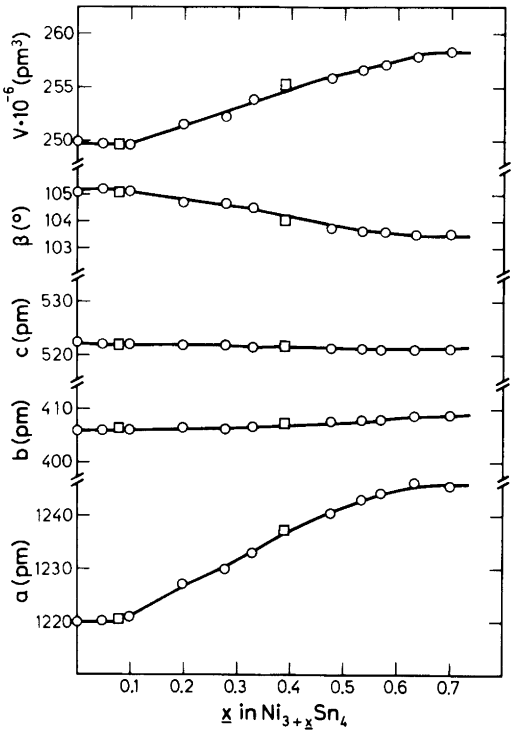

Fig. 1. Unit cell dimensions versus *x* for samples of $Ni_{3+x}Sn_4$ cooled slowly to room temperature. Squares represent data for single crystals.

Similar powder X-ray diffraction data were obtained for samples quenched from higher temperatures. Almost no change in the phase border with temperature is observed on the nickel-rich side of the homogeneity range. However, for temperatures above ~900 K there is an appreciable change in the border for tin-rich samples towards larger values of *x*, and at 1000 K the homogeneity range has shrunk to $0.40 \pm 0.04 \leqq x \leqq 0.52 \pm 0.04$.

High temperature powder X-ray diffraction data were collected for samples with nominal compositions corresponding to $x = 0.08$ and 0.39, respectively, between 300 and 900 K (Fig. 2). In this temperature range, the effect of the changes in the homogeneity range is negligible. The changes in the unit cell dimensions with temperature for $Ni_{3.08}Sn_4$ and $Ni_{3.39}Sn_4$ are seen to be very similar.

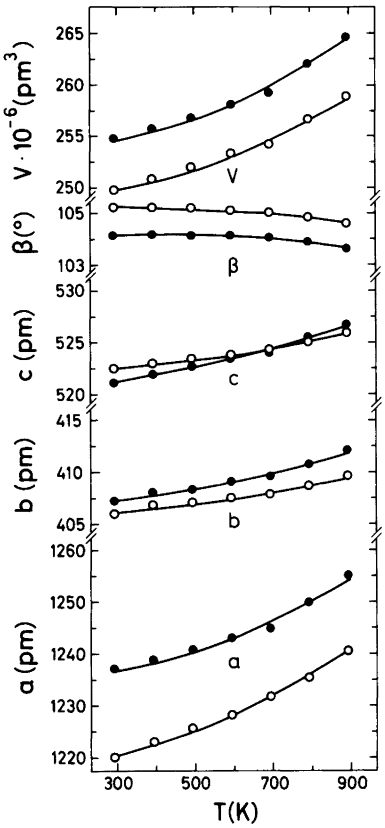

Fig. 2. Variation of unit cell dimensions with temperature between 300 and 900 K for $Ni_{3.08}Sn_4$ (○) and $Ni_{3.39}Sn_4$ (●).

The crystal structure of the $Ni_{3+x}Sn_4$ phase was refined for two single crystals having compositions with $x = 0.08$ and 0.39, respectively. The observed systematic extinctions comply with the requirements of the space group *C2/m*, and the positional parameters reported by Nowotny and Schubert[1] were used as starting values in the structure refinements. The tin atoms occupy two sets of 4(*i*) positions and the nickel atoms occupy 2(*a*) and 4(*i*) positions, respectively. However, as revealed from Fourier maps, the non-stoichiometry and the wide homogeneity range of the $Ni_{3+x}Sn_4$ phase is due to partial occupation of the 2(*c*) position by additional nickel atoms. The structure is shown in Fig. 3. Unit cell dimensions and some other characteristics are given in Table 1, and refined positional parameters together with thermal parameters are given in Table 2. The extent of occupancy of the 2(*c*) position was determined from the refinements, and the values obtained for the occupancy number, $g = 0.08 \pm 0.01$ and 0.39 ± 0.01, respectively, agree completely with the compositions $Ni_{3.08}Sn_4$ and $Ni_{3.39}Sn_4$ required by the unit cell dimensions. The low occupancy for Ni3 (see Table 2) in $Ni_{3.08}Sn_4$ did not permit an anisotropic temperature factor description for this atom. [Note that a completely filled 2(*c*) position implies composition NiSn.] As evident from Table 2, only minor changes in the positional parameters occur on changing the composition from $x = 0.08$ to $x = 0.39$. Interatomic separations up to 310 pm are listed for the two samples in Table 3.

The crystal structure of $Ni_{3+x}Sn_4$ (see Fig. 3) is,

Table 2a. Positional and thermal parameters for $Ni_{3.08}Sn_4$.

Atom	*x*	*y*	*z*	*U*
Ni1	.00000	.00000	.00000	.004
Ni2	.21455(6)	.00000	.33665(14)	.005
Sn1	.42849(3)	.00000	.68636(7)	.004
Sn2	.17184(3)	.00000	.81235(7)	.004
Ni3	.00000	.00000	.50000	.08(3)

Atom	*U*11	*U*22	*U*33	*U*12	*U*13	*U*23
Ni1	.0037(3)	.0039(4)	.0045(3)	.0000	.0011(3)	.0000
Ni2	.0058(2)	.0043(3)	.0042(2)	.0000	.0008(2)	.0000
Sn1	.0042(1)	.0035(1)	.0050(1)	.0000	.0004(1)	.0000
Sn2	.0043(1)	.0053(1)	.0038(1)	.0000	.0019(1)	.0000

Table 2b. Positional and thermal parameters for $Ni_{3.39}Sn_4$.

Atom	*x*	*y*	*z*	*U*
Ni1	.00000	.00000	.00000	.007
Ni2	.21259(10)	.00000	.33887(24)	.009
Sn1	.42633(5)	.00000	.69266(12)	.008
Sn2	.17480(6)	.00000	.81794(13)	.011
Ni3	.00000	.00000	.500000	.009

Atom	*U*11	*U*22	*U*33	*U*12	*U*13	*U*23
Ni1	.0045(5)	.0078(6)	.0067(5)	.0000	−.0002(4)	.0000
Ni2	.0088(4)	.0082(4)	.0078(4)	.0000	.0014(3)	.0000
Sn1	.0072(2)	.0070(2)	.0086(2)	.0000	−.0006(2)	.0000
Sn2	.0132(3)	.0098(2)	.0098(2)	.0000	.0060(2)	.0000
Ni3	.007(2)	.011(2)	.009(2)	.0000	−.001(1)	.0000

as pointed out by Bhargava and Schubert,[2] closely related to that of CoGe; the partially filled 2(*c*) site in $Ni_{3+x}Sn_4$ is fully occupied in CoGe.[7] When considering the crystal structure in more detail, similarities with other structure types also become evident. If one focuses on the surroundings of the Ni1 and Ni3 atoms, which are octahedrally (slightly distorted) coordinated by tin atoms, these form arrangements similar to that in the NiAs-type structure. However, the surroundings of the Ni2 atoms of $Ni_{3+x}Sn_4$ do not correspond to the NiAs-type, and they separate the NiAs-type related parts as indicated in Fig. 3. The Ni2 atoms form zig-zag chains (see Table 3) running parallel with the *b* axis. The coordination polyhedra around the Ni2 atoms consist of monocapped trigonal prisms. These are interconnected into columns running along the *b* direction, just as is found for $NiBi_3$.[8,9] For $Ni_{3+x}Sn_4$, the interconnected columns are linked together in the *c* direction by sharing faces, whereas they constitute separate units in $NiBi_3$. Similar considerations also apply to CoGe.

A completely vacant Ni3 position implies the composition $Ni_{3.0}Sn_4$, while completely filled implies $Ni_{4.0}Sn_4$. In this study, only occupancies between 0.08 and 0.60 have been observed. Rather short Ni3–Sn interatomic distances are observed, in particular for $Ni_{3.08}Sn_4$ (229.3 pm, see Table 3), and this is believed to reflect the partial occupancy of the Ni3 site. The variations in the Ni3–Sn distances as a function of *x* (data from Table 3, and calculated from data in Fig. 1 for assumed linear variation in the positional parameters with *x*) are shown in Fig. 4. The Ni–Sn average bond length is 259.3 and 269.7 pm for Ni1 and Ni2, respectively, whilst in Ni_2SnP the corresponding distance is 261.3 pm,[10] in NiSn 262.4 pm[2] and for the octahedrally coordinated Ni atoms in Ni_3Sn_2 269.8 pm.[11] From Fig. 4 it is seen that the short Ni3–Sn distance approaches a reasonable value when the occupancy approaches unity. A similar marked variation in interatomic distances is also found for other phases with large homogeneity ranges, e.g. Ni_tSn_2 with $2.7 \leqq t \leqq 3.3$[11] (for Ni in trigonal bipyramidal sites, the

Table 3. Interatomic distances (pm). Calculated standard deviations in parentheses.

Distance	$Ni_{3.08}Sn_4$	$Ni_{3.39}Sn_4$
Ni1 −Ni2 (×2)	274.2(1)	279.0(2)
Ni1 −Ni3 (×2)	260.9(1)	260.5(1)
Ni1 −Sn1 (×4)	261.2(1)	261.4(1)
Ni1 −Sn2 (×2)	253.5(1)	256.5(1)
Ni2 −Ni2 (×2)	264.5(1)	265.9(2)
Ni2 −Ni3 (×1)	295.6(1)	295.0(2)
Ni2 −Sn1 (×2)	265.7(1)	264.4(1)
Ni2 −Sn1 (×1)	276.4(1)	283.4(2)
Ni2 −Sn2 (×1)	264.8(1)	264.2(2)
Ni2 −Sn2 (×1)	266.7(1)	265.1(2)
Ni2 −Sn2 (×2)	268.4(1)	270.3(1)
Ni3 −Sn1 (×4)	250.3(1)	253.6(1)
Ni3 −Sn2 (×2)	229.3(1)	238.4(1)
Sn2−Sn2 (×2)	310.3(1)	308.1(1)

Ni–Sn distances increase from ~235 to ~239 pm). The introduction of additional Ni atoms into certain sites of such phases implies an increase in unit cell volume (the volume increments ascribed to these atoms amount to 6.0 and $8.8 \cdot 10^6$ pm^3 per atom for Ni_3Sn_2 and Ni_3S_2, respectively, while the present data for $Ni_{3+x}Sn_4$ yield a value of $7.1 \cdot 10^6$ pm^3).

The $Ni_{3+x}Sn_4$ phase is found to accept a maximum nickel content corresponding to $x = 0.60$. This suggests that the phase is not stable for more than ca. two-thirds occupancy of the Ni3 sites. However, for compositions $\sim 0.70 < x < \sim 0.78$ the NiSn phase is formed.[2] NiSn has a closely related crystal structure (with unit cell volume twice that of $Ni_{3+x}Sn_4$), and also exhibits partially occupied nickel positions. The structural characteristics discussed above for $Ni_{3+x}Sn_4$ are also found for NiSn. In NiSn the structural fragments related to the building blocks of the $NiBi_3$ type are partly connected via NiAs-type segments and partly via distorted NiAs-type segments. The nickel positions within the latter are completely filled, while vacancies occur in the former segment [confirmed by comparison of calculated and observed X-ray powder diffraction intensities (Guinier photographs; intensities obtained using a Nicolet L18 film scanner and the SCANPI programs[12])]. Hence, NiSn is more correctly described as $Ni_{7+y}Sn_8$. The range of existence is, according to Bhargava and Schubert,[2] restricted to $\sim 0.4 < y < \sim 0.55$, the nickel-poor limit being in good agreement with results of the present study. NiSn, or more precisely $Ni_{7.38}Sn_8$, also adopts short Ni–Sn distances[2] (239 pm), in agreement with the findings for Ni_3Sn_4 (Fig. 4). It is interesting to note that the Ni–Sn phases discussed do not attain a 1:1 composition, even though it seems quite possible from crystal structure considerations. However, a metastable NiSn (1:1) phase, prepared by electrolytic deposition, which crystallizes with the NiAs-type structure (a = 415 and c = 510 pm) has been reported,[13] the Ni–Sn distances (271.4 pm) being somewhat larger than commonly found for other nickel-tin phases.

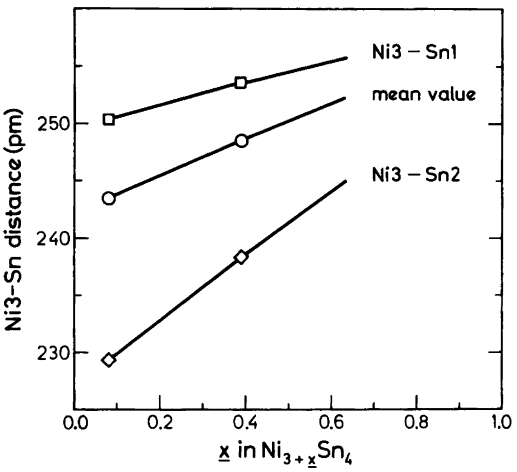

Fig. 4. Variation of Ni3–Sn interatomic distances with x for $Ni_{3+x}Sn_4$ (see text).

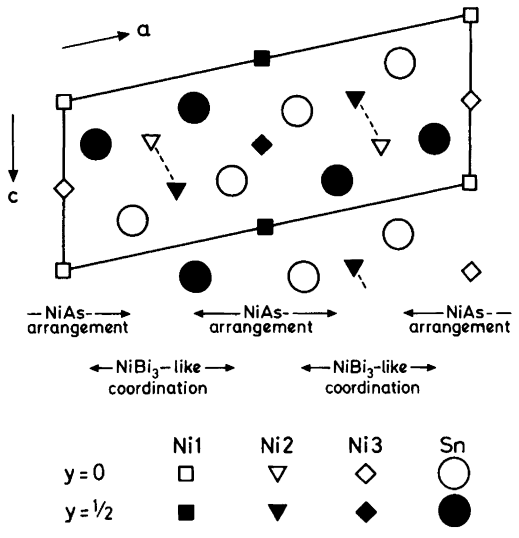

Fig. 3. Projection of the crystal structure of $Ni_{3+x}Sn_4$ on the *ac* plane. Ni–Ni zig-zag chains are indicated by dotted lines (see text).

Magnetic susceptibility measurements were made on samples of $Ni_{3+x}Sn_4$ with x = 0.15, 0.39 and 0.57. The $Ni_{3+x}Sn_4$ phase is weakly diamagnetic ($X_g = -0.02 \cdot 10^{-6}$ emu g^{-1} for x = 0.39 at 300 K), also after correction for core contributions, and the diamagnetic susceptibility increases with increasing value of x.

References

1. Nowotny, H. and Schubert, K. *Z. Metallkd. 37* (1946) 23.
2. Bhargava, M. K. and Schubert, K. *J. Less-Common Met. 33* (1973) 181.

3. Heumann, T. *Z. Metallkd. 35* (1943) 206.
4. Ersson, N. O. *Program CELLKANT,* Chemical Institute, Uppsala University, Uppsala, Sweden.
5. Groth, P. *Acta Chem. Scand. 27* (1973) 3131.
6. Mallinson, P. and Muir, K. W. *J. Appl. Crystallogr. 18* (1984) 51.
7. Bhan, S. and Schubert, K. *Z. Metallkd. 51* (1960) 327.
8. Glagoleva, V. P. and Zdanov, G. S. *Zh. Eksp. Teor. Fiz. SSSR. 26* (1954) 337.
9. Fjellvåg, H. and Furuseth, S. *J. Less-Common Met. In press.*
10. Furuseth, S. and Fjellvåg, H. *Acta Chem. Scand., Ser. A 39* (1985) 537.
11. Fjellvåg, H. and Kjekshus, A. *Acta Chem. Scand., Ser. A 40* (1986) 23.
12. Malmros, G. and Werner, P.-E. *Acta Chem. Scand. 27* (1973) 493.
13. Rooksby, H. P. *J. Electrodepositors Tech. Soc. 27* (1951) 153.

Received July 18, 1986.